JOURNAL OF MATERIALS SCIENCE 37 (2002) 2467–2474

Development of high strength magnesium based composites using elemental nickel particulates as reinforcement

S. F. HASSAN, M. GUPTA
Department of Mechanical Engineering, National University of Singapore, 10 Kent Ridge Crescent, Singapore 119260
E-mail: mpegm@nus.edu.sg

Magnesium based materials due to their inherently low density and ensuing potential to exhibit high specific mechanical properties are actively sought for weight-critical structural application. In the present study, elemental and nickel reinforced magnesium materials were synthesized using an innovative disintegrated melt deposition technique followed by hot extrusion. Microstructural characterization of the composite samples showed uniform distribution of nickel particulates in the matrix material, good interfacial integrity of magnesium matrix with nickel particulates and Mg-Ni based intermetallics, and the presence of minimal porosity. Physical properties characterization revealed that addition of nickel as reinforcement improves the dimensional stability of pure magnesium. Mechanical properties characterization revealed that the presence of nickel reinforcement lead to significant improvement in hardness, elastic modulus, 0.2% yield strength and UTS while the ductility was adversely affected. The results further revealed that the combination of 0.2% yield strength, UTS, and ductility exhibited by nickel reinforced magnesium remained much superior even when compared to high strength magnesium alloy AZ91 reinforced with much higher volume percentage of SiC. An attempt is made in the present study to correlate the effect of nickel as reinforcement and its increasing amount with the microstructural, physical and mechanical properties of magnesium.

1. Introduction

The increasing hostile service conditions that the modern engineering devices have to withstand have led the materials scientist across the globe to create new materials with enhanced properties when compared to the conventional materials. One way to improve the properties of conventional metallic materials is to reinforce them judiciously keeping the end application in mind. Among the reinforced metallic materials, magnesium based composites are becoming the strong candidates for lightweight structural application due to their superior specific mechanical properties. The use of high modulus and high strength reinforcements such as SiC particulates, for example, has been successful in overcoming some of the major limitations of monolithic magnesium such as low elastic modulus, rapid loss of strength with an increase in service temperature and poor creep resistance [1–6]. In addition, researchers have also reported an increase in dimensional stability and damping capacity of the magnesium matrices due to the presence of the SiC particulates [1–6].

Type of processing, matrix constitution, type, size, volume fraction and morphology of reinforcement, secondary processing and heat treatment are the common factors governing the end properties of a metal matrix composites [5, 7]. Judicial selection of reinforcing phase remains one of the most critical factors in developing a composite material with superior properties when compared to its monolithic counterparts. The results of literature search reveal that SiC is the most commonly investigated reinforcement in pure magnesium and commercial grade magnesium alloys with limited success in improving the overall mechanical properties specially the strength [1–6]. No investigation has been made so far to assess the feasibility of using stronger and stiffer metallic reinforcement to improve the properties of either pure magnesium or magnesium-based alloys.

Accordingly, the primary aim of the present study was to present preliminary results related to the microstructural, physical, and mechanical properties of pure magnesium reinforced with nickel particulates. The synthesis of materials was accomplished using an innovative disintegrated melt deposition (DMD) technique followed by hot extrusion. Particular emphasis was placed to assess the effect of presence of nickel as reinforcement and its increasing amount on the microstructure, physical and mechanical response of commercially pure magnesium matrix.

0022–2461

2. Experimental procedures

2.1. Materials

In this study, magnesium turnings of 99.9+% purity (supplied by ACROS Organics, New Jersy, USA) were used as the base material and elemental nickel particulates of 99.9% purity (Johnson Matthey, MA, USA) with an average size of 29 ± 19 μm were used as reinforcement phase.

2.2. Primary processing

Synthesis of monolithic and nickel reinforced magnesium composites (Mg/Nip) containing three different volume percentage of nickel reinforcement was carried out using (DMD) technique [8]. The synthesis of the composites involved superheating the magnesium turnings with reinforcement particulates (placed in multi-layer sandwich form) to 750°C under inert Ar gas atmosphere in a graphite crucible. Resistance heating furnace was used. The crucible was equipped with arrangement for bottom pouring. Upon reaching the superheat temperature, the molten slurry was stirred for eight minutes using a twin blade (pitch 45°) mild steel impeller to facilitate the incorporation and uniform distribution of reinforcement particulates in the metallic matrix, at 460 rpm. The impeller was coated with ZIRTEX 25 (86%-ZrO_2, 8.8% Y_2O_3, 3.6% SiO_2, 1.2% K_2O & Na_2O and 0.3% trace inorganic) to avoid iron contamination to the molten metal. The melt was then released through a 10 mm diameter orifice at the base of the crucible. The composite melt was disintegrated by two jets of argon gas orientated normal to the melt stream and located 265 mm from the melt pouring point. The argon gas flow rate was maintained at 251/min. The disintegrated composite melt slurry was subsequently deposited onto a metallic substrate located 500 mm from the disintegration point. Ingot of 40 mm diameter was obtained following the deposition stage. The synthesis of monolithic magnesium was carried out using steps similar to those employed for the reinforced materials except that no reinforcement particulates were added.

2.3. Secondary processing

The deposited monolithic and nickel reinforced magnesium ingots were machined to 36 mm diameter and hot extruded using an extrusion ratio of 20.25 : 1 on a 150-ton hydraulic press. Extrusion temperatures were used as 350°C for Mg/7.3Ni_P and Mg/14.0Ni_P, and 400°C for Mg/24.9Ni_P composites, respectively. Mg/24.9Ni_P was extruded at 400°C as it could not be extruded at 350°C. The ingots were heated at 400°C for 50 minutes in a constant temperature furnace before extrusion. Colloidal graphite was used as lubricant. Rods of 8 mm diameter were obtained following extrusion.

2.4. Quantitative assessment of nickel

Quantitative assessment of retained nickel in extruded composites was conducted by inductively plasma atomic emission method using inductively coupled plasma spectrometer (Thermo Jarrell Ash, IRIS AP Duo OES). This method involved: (a) dissolving a known amount of sample in the nitric acid, (b) atomizing the solution into plasma, and (c) analyzing the plasma in the inductively coupled plasma spectrometer, which detects the wavelength of nickel. Tests were carried out on specimens randomly selected from at least three different points of extruded rod of each composite.

Image analysis using Quantimet 520 image analysis system was used to determine the size and amount of unreacted nickel in the magnesium matrix. The procedure involved digitizing the scanning electron micrographs into binary images followed by cumulative analysis of all the images. A total of fifteen most representative scanning electron micrographs for each Mg/Ni_P composite were used for the purpose of image analysis.

2.5. Density measurements

Density (ρ) measurements were performed on polished samples of Mg and Mg/Ni_P taken from extruded rods. This was carried out in accordance with Archimedes' principle [1, 8]. Distilled water was used as the immersion fluid. The samples were weighed using an A&D ER-182A electronic balance, with an accuracy of ± 0.0001 g.

2.6. Microstructural characterization

Microstructural characterization studies were conducted on composites to investigate reinforcement distribution, interfacial integrity between the matrix and reinforcement, and the presence of porosity. JEOL JSM-5800 LV Scanning Electron Microscope (SEM) equipped with Energy Dispersive Spectroscopy (EDS) was used. The extruded composites samples were metallographically polished prior to examination.

Image analysis using Quantimet 520 image analysis system was used to determine volume percentage of porosity in extruded composite material. A total of fifteen most representative scanning electron micrographs for each composite material were used for image analysis.

2.7. X-ray diffraction studies

Extruded Mg and Mg/Ni_P samples were exposed to Cu K_α radiation ($\lambda = 1.5418$ Å) with a scan speed of 2 deg/min on an automated Shimadzu LAB-X XRD-6000 diffractometer. The Bragg angles and the values of interplanar spacing, d, obtained were subsequently matched with standard values [9] for Mg, Ni, Mg_2Ni and other related phases.

2.8. Coefficient of thermal expansion

The coefficients of thermal expansion (CTE) of the extruded Mg and composites samples were determined using an automated SETARAM 92-16/18 thermomechanical analyzer. Displacement of the monolithic Mg and Mg/Ni_P composites samples (8 mm diameter and thickness of about 15 mm) as a function of temperature (50–400°C) was measured using an alumina probe under argon atmosphere and was subsequently used to determine the CTE. The heating rate employed was 5°C/min while argon gas flow rate was maintained at 1.2 l/min.

2.9. Mechanical behavior

Microhardness and macrohardness measurements were made on the polished Mg and Mg/Ni$_P$ samples. Vickers microhardness was measured by Matsuzawa MXT50 automatic digital microhardness tester using 25 gf indenting load, 50 μm/s indentation rate and 15 seconds dwell time. Rockwell 15T superficial scale was used for macrohardness measurement in accordance with ASTM E18-94 standard.

The smooth bar tensile properties of the extruded Mg and Mg/Ni$_P$ samples were determined in accordance with ASTM test method E8M-96. The tensile tests were conducted on round tension test specimens of diameter 5 mm and gauge length 25 mm using Instron 8516 machine with a crosshead speed set at 0.254 mm/min.

2.10. Fracture behavior

Fracture surface characterization studies were carried out on the tensile fractured surfaces of the Mg and Mg/Ni$_P$ samples to provide insight into the fracture mechanisms operative during tensile loading. Fractography was accomplished using a JEOL JSM-5800 LV SEM equipped with EDS.

3. Results

3.1. Macrostructure

The result of macrostructural characterization conducted on the as deposited unreinforced and composites samples did not reveal any presence of macropores in the matrix. Solidification shrinkage cavity was absent in as-cast ingots. Following extrusion, there was also no evidence of any macrostructural defects.

3.2. Quantitative assessment of nickel

Result of inductively coupled plasma spectrometer showed successful retention of nickel in the extruded composite matrices. The results of image analysis revealed the presence of nickel particulates in the unreacted form distributed uniformly in the magnesium matrix. Image analysis also showed the reduction in the size of elemental nickel particulates in the extruded composites. Results are shown in Table I.

3.3. Density measurement

The results of the density measurements conducted on extruded Mg and Mg/Ni$_P$ samples are shown in Table I. The results indicate that near dense materials can be obtained using the fabrication methodology adopted in the present study.

3.4. Microstructural characterization

Scanning electron microscopy conducted on the extruded composites specimens shows distribution pattern of unreacted and reacted nickel and the presence of minimal porosity (see Fig. 1). Fig. 2 shows a typical scanning electron micrograph illustrating Ni$_P$/Mg interfacial characteristics with the corresponding EDS area maps. The interface of nickel particulates with the magnesium matrix did not reveal the presence of debonded areas or the voids.

3.5. X-Ray diffraction studies

The X-ray diffraction results corresponding to the Mg and Mg/Ni$_P$ samples were analyzed. The lattice spacing (d) obtained was compared with standard values for Mg, Ni, Mg_2Ni and various phases of the Mg-O and Ni-O systems. The detailed results of the phase analysis are shown in Table II.

3.6. Coefficient of thermal expansion

The results of CTE measurements obtained from extruded monolithic and reinforced magnesium composites samples are listed in Table II. The results show the improvement in dimensional stability of magnesium matrix with increase in weight percentage of nickel in the temperature range of 50–400°C.

3.7. Mechanical behavior

The results of the microhardness and macrohardness measurements conducted on extruded Mg and Mg/Ni$_P$ samples revealed significant increment in hardness value with an increasing weight percentage of nickel in magnesium matrix. (see Table III). The microhardness of the Mg-Ni$_P$ interfacial region in the case of Mg/Ni$_P$ samples were found to be higher when compared to that of the matrix region.

The results of ambient temperature tensile tests revealed that the addition of nickel as reinforcement led

TABLE II Results of X-ray diffraction studies and coefficient of thermal expansion analysis

Materials	Number of matching peaks					CTE ($\times 10^{-6}$/°C)
	Mg	Ni	Mg_2Ni	NiO	Ni_2O_3	
Mg	9 [3]	–	–	–	–	28.60 ± 0.07
Mg/7.3Ni$_P$	6 [3]	–	6 [2]	–	–	27.54 ± 0.26
Mg/14.0Ni$_P$	5 [3]	–	8 [2]	–	–	26.35 ± 0.09
Mg/24.9Ni$_P$	6 [3]	2 [1]	16 [2]	1 [1]	1	20.75 ± 0.56

[ ] indicates the number of main peaks matched.

TABLE I Results of density and porosity measurements

Material	Reinforcement in composites				Density (g/cm^3)	Porosity (vol%)
	(wt%)	(vol%)[a]	(vol%)[b]	Size[c]		
Mg	–	–	–	–	1.7395 ± 0.0005	0.05
Mg/7.3Ni$_P$	7.3	1.5	0.1	2.7 ± 0.6	1.9046 ± 0.0038	0.12[c]
Mg/14.0Ni$_P$	14.0	3.1	1.3	2.5 ± 0.4	2.0677 ± 0.0002	0.02[c]
Mg/24.9Ni$_P$	24.9	6.1	4.3	9.0 ± 4.6.	2.3834 ± 0.0092	0.55[c]

[a]Computed by using the total amount of Ni retained in composite samples.
[b]Indicates the amount of Ni in the unreacted form present in composite samples.
[c]Result of cumulative image analysis conducted on fifteen representative SEM micrographs for each composite.

TABLE III Results of microhardness and macrohardness measurements

Materials	Microhardness (HV)		Macrohardness (HR15T)
	Matrix	Interface	
Mg	43 ± 0	–	57 ± 1
Mg/7.3Ni$_P$	65 ± 2	74 ± 3	69 ± 1
Mg/14.0Ni$_P$	78 ± 1	108 ± 6	79 ± 1
Mg/24.9Ni$_P$	102 ± 3	121 ± 5	82 ± 1

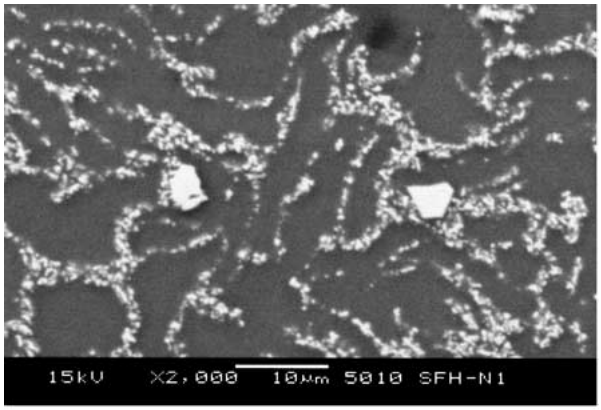

(a)

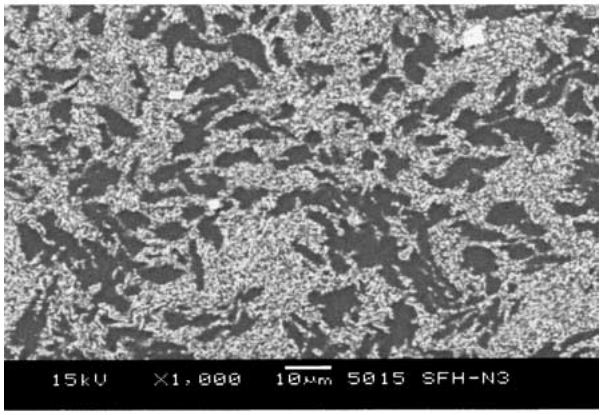

(b)

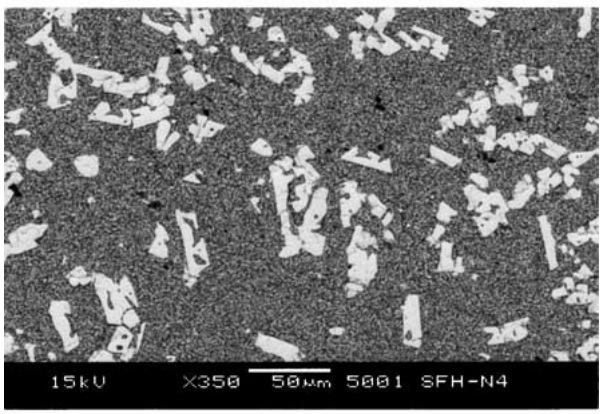

(c)

Figure 1 Representative SEM micrographs showing distribution of nickel and its reaction product in: (a) Mg/7.3Ni$_P$, (b) Mg/14.0Ni$_P$ and (c) Mg/24.9Ni$_P$ matrices.

to significant increments in elastic modulus of magnesium matrix (see Table IV). The results also revealed the similar trend of superiority in 0.2% yield strength and UTS in composites with nickel up to 14.01 weight percentage. In the case of Mg/24.9Ni$_P$ composite failure strength remained higher (21%) when compared with unreinforced magnesium but the ductility was significantly compromised. The ductility of magnesium matrix, in general, was adversely affected with the presence and increasing amount of reinforcement.

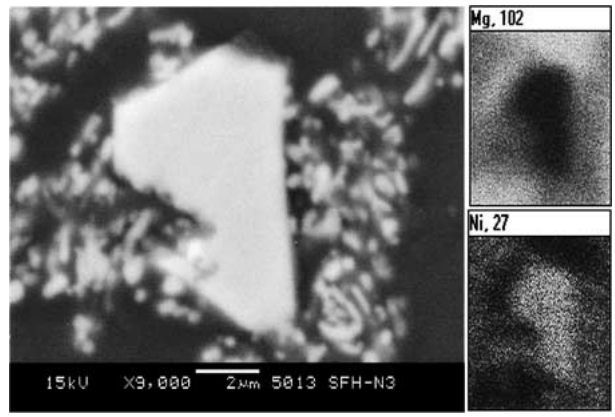

Figure 2 Representative SEM micrograph showing the typical interfacial characteristics of Ni$_P$-Mg interface in Mg/14.0Ni$_P$ composite with EDS area maps.

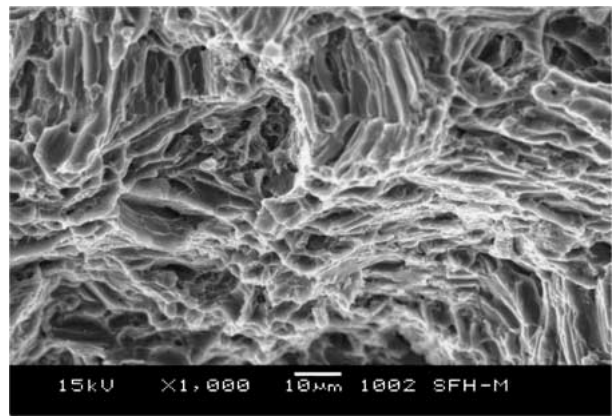

Figure 3 Representative SEM micrograph taken from the tensile fracture surface of pure Mg showing cleavage marks indicative of brittle fracture.

3.8. Fracture behavior

The tensile fracture surfaces of Mg and Mg/Ni$_P$ samples are shown in Figs 3–5. The fracture surface of the pure Mg samples indicates a cleavage type of failure mode (see Fig. 3). Fracture studies conducted on the Mg/Ni$_P$ samples revealed mixed-mode type of fracture exhibiting matrix deformation (see Fig. 4) and breakage of Ni$_P$ (see Fig. 5a and b). In addition, micro-cracks were also observed in the matrix of Mg/Ni$_P$ samples (see Fig. 5c).

4. Discussion

4.1. Synthesis of Mg and Mg/Ni$_P$ materials

Synthesis of Mg and Mg/Ni$_P$ materials was successfully accomplished using the methodology of DMD process followed by hot extrusion. Important features revealed in present study are: (a) minimal oxidation of magnesium, (b) absence of macropores and blowholes, and (c) no detectable reaction between Mg or Mg/Ni$_P$ melts and the graphite crucible.

TABLE IV Results of room temperature tensile properties

Materials	Reinforcement (Vol%)	E (GPa)	0.2% YS (MPa)	UTS (MPa)	Ductility (%)	$\sigma_{0.2\%\,YS}/\rho$	σ_{UTS}/ρ
Mg	–	43 ± 1	100 ± 4	258 ± 16	7.7 ± 1.2	58	148
Mg/7.3Ni$_P$	1.5 (0.1)[a]	47 ± 1	337 ± 15	370 ± 14	4.8 ± 1.4	177	194
Mg/14.0Ni$_P$	3.1 (1.3)[a]	53 ± 1	420 ± 27	463 ± 4	1.4 ± 0.1	203	224
Mg/24.9Ni$_P$	6.1 (4.3)[a]	58 ± 1	–	313 ± 29[b]	0.7 ± 0.1	–	131
Mg [10]	–	44	69–105	165–205	5–8	–	–
Mg/SiC$_P$ [2]	30	59	229	258	2	105[c]	118[c]
AZ91D/SiC$_P$ [3]	10	44.7	135	152	0.8	69[d]	77[d]
AZ91D/SiC$_P$ [4]	15	64.5	257	289	0.7	126[d]	142[d]

[a]Value refer to nickel in both unreacted and reacted form while numbers in parentheses refers to nickel in unreacted form.
[b]Refer to the failure stress.
[c]Density value of 2.19 g/cm^3 was given.
[d]Density value was calculated by taking 1.83 g/cm^3 and 3.21 g/cm^3 as density of AZ91 [11] and SiC [12] respectively and assuming zero porosity in composite.

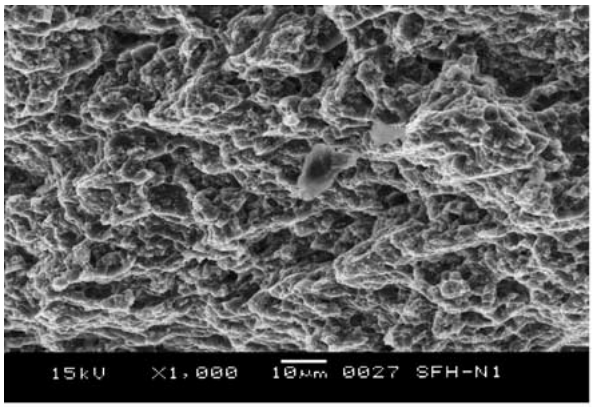

(a)

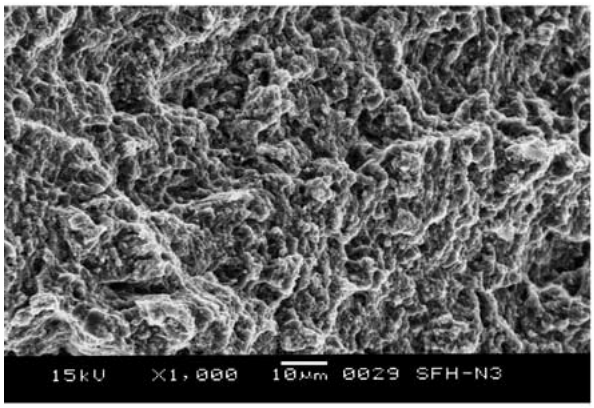

(b)

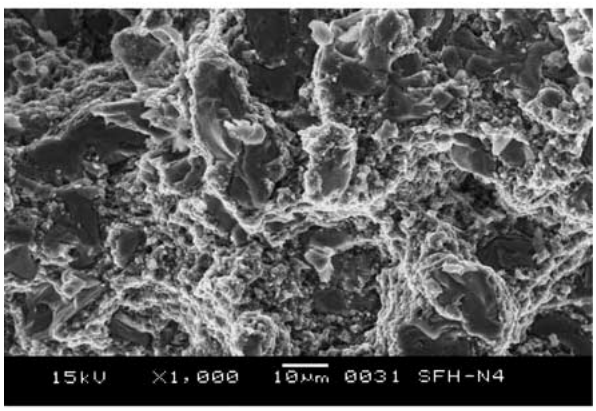

(c)

Figure 4 Representative SEM micrographs taken from the tensile fracture surface of composites showing typical matrix deformation of: (a) Mg/7.3Ni$_P$, (b) Mg/14.0Ni$_P$ and (c) Mg/24.9Ni$_P$.

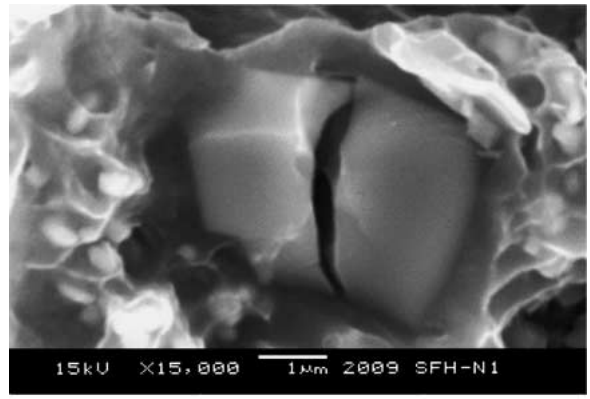

(a)

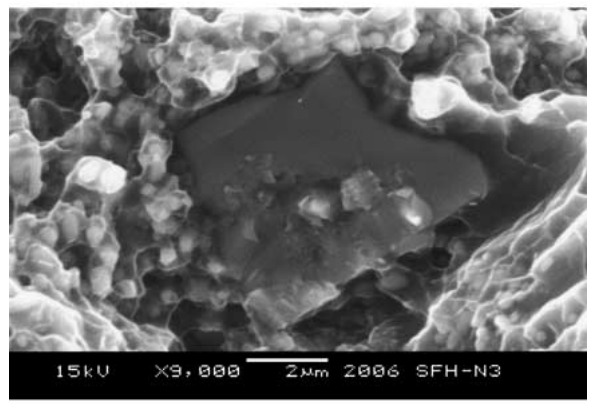

(b)

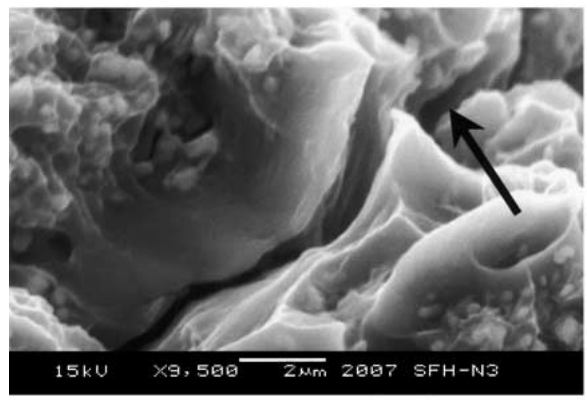

(c)

Figure 5 Representative SEM micrographs taken from the tensile fracture surface of composites showing: (a) and (b) fractured Ni particulates in the case of Mg/7.3Ni$_P$ and Mg/14.0.3Ni$_P$, and (c) presence of a microcrack in matrix of Mg/14.0Ni$_P$ composite (marked by arrow).

The inert atmospheric condition used during melt processing, dispersion, deposition/solidification was instrumental in the prevention of reaction between air/oxygen and Mg melt. The absence of macro-pores, blowholes, and segregation or agglomeration of reinforcement particulates due to the effect of gravity indicates the suitability of stirring conditions in the crucible and the realization of good solidification conditions during deposition. The absence of macro-pores and blowholes also suggests that, the continuous flow of argon during the melting, stirring and deposition process did not lead to the entrapment of gases. The absence of reaction between Mg and Mg/Ni_P with the graphite crucible suggests that the temperature-time cycle used during the synthesis process was insufficient to trigger the reaction. The absence of reaction with the graphite crucible can also be attributed to the inability of magnesium to form stable carbides [3, 5]. The results, in essence, indicate the feasibility of DMD process as a potential fabrication technique for Mg and Mg/Ni_P MMCs.

4.2. Microstructure

The results of the microstructural characterization studies conducted on the extruded Mg and Mg/Ni_P samples are discussed in terms of: (a) size of the nickel particulates and distribution of the nickel particulates and Mg-Ni reaction product, (b) reinforcement—matrix interfacial characteristics, and (c) the presence of porosity.

The result of image analysis for quantitative assessment of elemental nickel in composites revealed that the processing methodology used in this present study reduced the average size of nickel particulates (see Table I). Severe reaction between magnesium melt and nickel particulates during DMD processing led to the reduction of the particulate size and formation of Mg_2Ni intermetallics [13]. The results of quantitative determination of unreacted nickel (see Table I), microstructural characterization illustrating the presence of reaction products (see Fig. 1) and XRD results (see Table II) showing the presence of Mg_2Ni supports the experimental observations. It may be noted that the elemental Ni in Mg/7.3Ni_P and Mg/14.0Ni_P composites microstructure was not detected in XRD results due to the limitation of filtered X-ray radiation to detect the phases with less than two volume percent in a multiphase structure [14].

The results of scanning electron microscopy revealed a uniform distribution of nickel particulates in magnesium matrix (see Fig. 1). This can be attributed to: (a) minimal agglomeration of reinforcement during melting of matrix due to discreet arrangement of raw materials in crucible for melting. It may be noted that thin layers of nickel particulates were placed between magnesium turnings in sandwich form, (b) good wetting of reinforcement by the matrix melt [15], (c) minimal gravity-associated segregation due to judicious selection of stirring parameters which ensured uniform incorporation of Ni particulates in matrix melt, and (d) disintegration of the composite slurry by argon jets and its subsequent deposition in metallic mold.

The results of microstructural characterization obtained from composite materials also revealed a near-defect free interface formed between reinforcement and matrix (see Fig. 2). The interfacial integrity was assessed in terms of interfacial debonding and presence of microvoids at the particulate-matrix interface. The results of EDS area mapping revealed the presence of nickel enrichment adjacent to the Ni particulate corresponding to the bright intermetallic precipitates. A typical SEM micrograph taken from Mg/14.0Ni_P composite material along with EDS area map is shown in Fig. 2. The results indicate that the temperature and time conditions selected during processing permitted reasonable chemical interaction between Ni particulates and Mg melt. These bright phases are most likely Mg_2Ni phases as revealed by XRD results (see Table II).

The results of image analysis also revealed the presence of minimal porosity in Mg/Ni_P composite materials (see Table I). This can be attributed to: (a) realization of good solidification conditions during the deposition stage, (b) good compatibility between Mg matrix, Ni_P and Mg_2Ni [13, 15] during solidification leading to the absence of voids and debonded regions normally associated with the reinforcement-matrix interface, and (c) the use of an appropriate extrusion ratio. It has been established convincingly in the earlier studies, the ability of an extrusion ratio even as low as 12 : 1 to nearly close the micrometer-size porosity associated with as-solidified metal-based materials [1, 5, 8].

4.3. Coefficient of thermal expansion

The results of CTE measurements in the temperature range of 50–400°C revealed that the presence of an increasing percentage of nickel reduces the CTE value of magnesium matrix (see Table II). This can be attributed to: (a) lower coefficient of thermal expansion of nickel (27.0×10^{-6}/°C and 13.9×10^{-6}/°C for Mg and Ni [11], respectively), (b) uniform distribution of reinforcement particulates, and (c) good interfacial integrity between reinforcement and matrix. It may be noted that the reduction of the CTE of the matrix can also be attributed to the presence of Mg_2Ni phase. Such a correlation, however, is not attempted in this study due to the unavailability of CTE of Mg_2Ni in the open literature. The results obtained in the present study indicate the feasibility of using nickel particulates in enhancing the dimensional stability of magnesium matrix.

4.4. Mechanical behavior

The significant increment in microhardness and macrohardness (see Table III) of Mg matrix with the increase in weight percentage of reinforcement can be attributed primarily to: (a) the presence of relatively harder intermetallic phase and elemental Ni particulates in the matrix (see Tables I and II) [1, 11, 16], and (b) a higher constraint to the localized matrix deformation during indentation due to their presence. It may be noted that intermetallics are extremely hard relative to their pure components [16]. Higher concentration of reaction product may lead to further increment of microhardness in the near vicinity of particulates. It may be noted that hardness results obtained in the present

study are similar to the findings reported for ceramic reinforced magnesium matrices [1, 2].

The elastic modulus measurement revealed that increase in the weight percentage of nickel leads to significant increase in elastic modulus of magnesium matrix (see Table IV). Increase in modulus was expected due to: (a) the presence of reinforcement with high modulus (i.e., 199.5 GPa for Ni [11]), and (b) uniform distribution of reinforcement with good interfacial integrity. It may be noted that uniform distribution of reinforcement coupled with good matrix-reinforcement interfacial integrity lead to a significant increase in internal stress between reinforcement and matrix resulting in the enhancement of elastic modulus [3]. It may also be noted that the increase in elastic modulus may also partly be attributed to the presence of Mg_2Ni. However, further work may be required to establish this point due to lack of information in open literature about the mechanical characteristics of Mg_2Ni.

The results of tensile properties characterization (see Table IV) also revealed that the Mg/7.3Ni_P and Mg/14.0Ni_P samples exhibited a significant increase in 0.2% YS and UTS when compared to the pure magnesium samples. The remarkable increase in 0.2% YS and UTS of Mg matrix due to addition of nickel as reinforcement can primarily be attributed to: (a) the presence of uniformly distributed elemental Ni particulates coupled with the strengthening effect of Mg_2Ni, [16] and (b) effective transfer of applied tensile load to the uniformly distributed and well-bonded high strength reinforcement (0.2% YS and UTS are 200 MPa and 500 MPa [11] respectively, for hot rolled 99% purity commercial grade Ni). These microstructural characteristics assist in uniform distribution of the applied load across the composite microstructure and minimize stress concentration sites [7]. In the case of Mg/24.9Ni_P composite, the failure stress was higher than that of 0.2% YS and UTS of pure magnesium but remained lower than that of Mg/7.3Ni_P and Mg/14.0Ni_P composites. This suggests that the best tensile properties can be realized for Mg-Ni formulation only for a threshold amount of nickel in the matrix. Further work is ongoing to identify the factors responsible for the decrease in 0.2% YS and UTS of magnesium when the amount of the nickel in the matrix was increased from 14.0% to 24.9%.

Compared to Mg samples, ductility of composites reduced with increasing amount of nickel. The reduction in ductility of Mg/Ni_P composites can be attributed mainly to the presence of higher volume fraction of brittle intermetallics, Mg_2Ni, at the particle matrix interface as well as in the matrix [17]. It may be noted that the presence of harder phases in the matrix lead to the plastic incompatibility and thus serves as crack nucleation sites leading to the reduction in ductility under the action of uniaxial tensile load [18].

The results further revealed that both engineering and specific 0.2% YS and UTS, and ductility of Mg/7.3Ni_P and Mg/14.0Ni_P composites remained much superior even when compared to the high strength magnesium alloy AZ91 reinforced with much higher volume percentage of SiC_P (see Table IV).

4.5. Fracture behavior

The results of fracture analysis revealed typical brittle fracture in the case of Mg samples (see Fig. 3). This can be attributed to the HCP crystal structure of Mg that restricts the slip to the basal plane. The presence of small steps and microscopically rough fracture surface indicates the inability of magnesium to cleave on any single plane. These findings are consistent with those reported elsewhere [19].

In the case of Mg/Ni_P samples, the areas exhibiting extensive plastic deformation adjacent to the Ni particulates are indicative of strain accumulation at the interfacial zone (see Fig. 4). The presence of broken Ni particulates (see Fig. 5a and b) with no evidence of interfacial debonding indicates that a strong interfacial bond was realized between the Ni particulates and the magnesium matrix using the present experimental methodology. Crack propagation in matrix through micro-void coalescence, initiated by particulate cracking, is indicative of effective load transfer to particulates [20]. In addition, micro-cracks observed in the matrix indicate that the failure might have initiated in the matrix rather than from particulates (see Fig. 5c). This is also indicative of strong Ni_P/Mg interfacial [21] integrity realized in the composites synthesized in the present study.

5. Conclusions

The primary conclusions that may be derived from this work are as follows:

1. Disintegrated melt deposition technique coupled with hot extrusion can be used to synthesize monolithic and elemental nickel reinforced magnesium.
2. The uniform distribution of Ni particulates, strong Ni_P-Mg interfacial integrity and the presence of minimal porosity in the composite microstructure indicate the suitability of primary processing and secondary processing parameters used in the present study.
3. Results of coefficient of thermal expansion measurement indicate that the increasing presence of nickel is able to improve the dimensional stability of pure magnesium.
4. The results of mechanical characterization revealed that the increasing presence of nickel (in elemental/intermetallic form) lead to a significant improvement in hardness and stiffness. Improvement in 0.2% yield strength and ultimate tensile strength of magnesium was realized for nickel weight percentage limiting to 14.0. The ductility of the magnesium matrix was found to decrease with an increasing amount of nickel.
5. The results of fracture surface characterization of Mg/Ni_P composites revealed that particle breakage is the dominating reinforcement-associated failure mechanism under tensile loading.

References

1. M. GUPTA, M. O. LAI and D. SARAVANARANGANATHAN, *J. Mater. Sci.* **35** (2000) 2155.
2. R. A. SARAVANAN and M. K. SURAPPA, *Mater. Sci. Eng.* A **276** (2000) 108.

3. A. LUO, *Metall. Trans.* A **26** (1995) 2445.
4. V. LAURENT, P. JARRY, G. REGAZZONI and D. APELIAN, *J. Mater. Sci.* **27** (1992) 4447.
5. D. J. LLOYD, *Int. Mater. Rev.* **39**(1) (1994) 1.
6. S. GULDBERG, H. WESTENGEN and D. L. ALBRIGHT, Technical Paper 910830 (SAE, Warrendale, PA, USA, 1990) p. 1.
7. P. KELLEY, *Composites* **10** (1979) 2.
8. L. M. THAM, M. GUPTA and L. CHENG, *Mater. Sci. Tech.* **15** (1999) 1139.
9. Powder Diffraction File, International Center for Diffraction Data (1601 Park Lane, Swarthmore, PA, USA, 1991).
10. "ASM Handbook: Properties and Selection: Non-Ferrous Alloys and Special-Purpose Materials," Vol. 2 (ASM International, Materials Park, OH, 1990) p. 1134.
11. C. J. SMITHELLS, in "Metals Reference Book" 7th edn. (Butterworth-Heinemann Ltd, London, 1992) pp. 14-2, 14-19, 15-3 and 22-71.
12. J. F. SHACKELFORD, W. ALEXANDER and J. S. PARK, in "CRC Materials Science and Engineering Handbook," 2nd edn. (CRC Press, 1994) p. 50.
13. A. A. NAYEB-HASHEMI and J. B. CLARK, in "Phase Diagram of Binary Magnesium Alloys" (ASM International Publication, USA, 1988) p. 219.
14. B. D. CULLITY, in "Element of X-Ray Diffraction," 2nd edn. (Addison-Wesley Publishing Comp. Reading, MA, 1978) p. 414.
15. N. EUSTATHOPOULOS, M. G. NICHOLAS and B. DREVET, in "Wettability at High Temperatures" Pregamon Materials Series, Vol. 3 (Elsevier Science Ltd, UK, 1999) p. 175 and 187.
16. J. H. WESTBROOK, in "Intermetallic Compounds" (John Wiley & Sons, New York, 1967) p. 11 and 471.
17. G. F. BOCCHINI, *Int. J. Powder Metall.* **22**(3) (1986) 185.
18. M. GUPTA, *Aluminum Trans.* **1**(1) (1999) 33.
19. R. E. REED-HILL, in 'Physical Metallurgy Principles," 2nd edn. (Van Nostrand, New York, 1973) p. 753.
20. R. W. CAHN and P. HAASEN, in "Physical Metallurgy" (North-Holland Physics Publishing, New York, USA, 1983) p. 1862.
21. V. V. BHANUPRASHAD, M. A. STALEY, P. RAMAKRISHNAN and Y. R. MAHAJAN, *Key Engn. Mater.* **104–107** (1995) 495.

Received 14 June 2001
and accepted 12 February 2002